

# Assessing the impact of interannual variability of precipitation and potential evaporation on evapotranspiration



Dan Li <sup>\*,1</sup>

Department of Civil and Environmental Engineering, Princeton University, Princeton, NJ 08540, USA

## ARTICLE INFO

### Article history:

Received 6 August 2013

Received in revised form 1 April 2014

Accepted 17 April 2014

Available online 26 April 2014

### Keywords:

Budyko

Evapotranspiration

Precipitation

Potential evaporation

Interannual variability

Stochastic soil moisture model

## ABSTRACT

The impact of interannual variability of precipitation and potential evaporation on the long-term mean annual evapotranspiration as well as on the interannual variability of evapotranspiration is studied using a stochastic soil moisture model within the Budyko framework. Results indicate that given the same long-term mean annual precipitation and potential evaporation, including interannual variability of precipitation and potential evaporation reduces the long-term mean annual evapotranspiration. This reduction effect is mostly prominent when the dryness index (i.e., the ratio of potential evaporation to precipitation) is within the range from 0.5 to 2. The maximum reductions in the evaporation ratio (i.e., the ratio of evapotranspiration to precipitation) can reach 8–10% for a range of coefficient of variation (CV) values for precipitation and potential evaporation. The relations between the maximum reductions and the CV values of precipitation and potential evaporation follow power laws. Hence the larger the interannual variability of precipitation and potential evaporation becomes, the larger the reductions in the evaporation ratio will be. The inclusion of interannual variability of precipitation and potential evaporation also increases the interannual variability of evapotranspiration. It is found that the interannual variability of daily rainfall depth and that of the frequency of daily rainfall events have quantitatively different impacts on the interannual variability of evapotranspiration; and they also interact differently with the interannual variability of potential evaporation. The results presented in this study demonstrate the importance of understanding the role of interannual variability of precipitation and potential evaporation in land surface hydrology under a warming climate.

© 2014 Elsevier Ltd. All rights reserved.

## 1. Introduction

Climate fluctuations such as the seasonal and interannual variability of precipitation play important roles in affecting the terrestrial hydrology and vegetation dynamics [1–4]. For example, studies have shown that the temporal variability of precipitation has profound impacts on tropical forests [5,6] and arid/semiarid ecosystems [7,8]. Understanding the impact of these climate fluctuations is extremely important, especially under a changing climate where these fluctuations may be modulated [9–11]. Recognizing the importance of climate variability, the Intergovernmental Panel on Climate Change (IPCC) calls for more research to document its change and assess its impacts [12].

This study aims to study the impact of interannual variability of precipitation and potential evaporation on evapotranspiration due

to the central role of evapotranspiration in the hydrological cycle and in the surface energy balance [13–15]. Evapotranspiration is also closely linked to ecosystem productions [16,17]. In this study, the focus is on the long-term mean annual evapotranspiration as well as the interannual variability of evapotranspiration. The long-term mean annual evapotranspiration is usually recognized as to be controlled by water availability (usually represented by the long-term mean annual precipitation) and energy availability (usually represented by the long-term mean annual potential evaporation) [18–22]. A semi-empirical curve that describes the relationship between the long-term mean annual precipitation ( $P$ ), potential evaporation ( $E_p$ ), and evapotranspiration ( $E_e$ ) is called the Budyko curve (see Fig. 1). The ratio of  $E_p/P$  is called the dryness index and the ratio of  $E/P$  is called the evaporation ratio hereafter. Note that  $E/P$  is called evaporation ratio instead of evapotranspiration ratio in order to follow the convention. The Budyko curve has been widely used to study the impact of climate change on the terrestrial hydrological cycle at annual and long-term scales [23–29].

Using the Budyko framework and assuming that annual precipitation, potential evaporation, and evapotranspiration also satisfy

\* Tel.: +1 6099372644.

E-mail address: [danli@princeton.edu](mailto:danli@princeton.edu)

<sup>1</sup> Now in the Program of Atmospheric and Oceanic Sciences at Princeton University, Princeton, NJ 08540, USA.

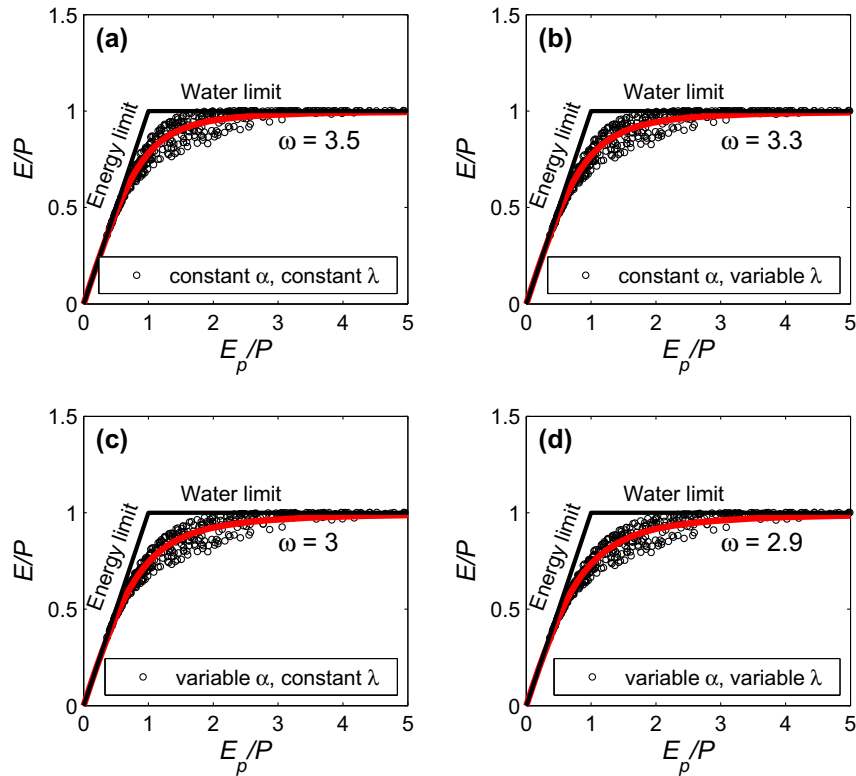


**Fig. 1.** The long-term mean annual evaporation ratios ( $E/P$ ) are shown as a function of the long-term mean annual dryness index ( $E_p/P$ ). When the daily rainfall depth ( $\alpha$ ) and the frequency of daily rainfall events ( $\lambda$ ) are variable, their CV values are set to be 0.35 and 0.21, respectively. Other parameters are specified in Table 1. Each dot here represents one basin with a distinct pair of mean ( $\alpha$ ,  $\lambda$ ) and there are 500 pairs of mean ( $\alpha$ ,  $\lambda$ ). The bold black lines serve as an envelope (energy limit and water limit) for the long-term water and energy balances. The Budyko curve is shown as the black line, which is calculated from Fu's equation (see Eq. (8)) with  $\varpi$  fitted to the data.

the Budyko curve, Koster and Suarez [30] derived an analytical expression for the interannual variability of evapotranspiration ( $\sigma_E$ ), which is a function of the dryness index ( $E_p/P$ ), the interannual variability of precipitation ( $\sigma_P$ ), and the interannual variability of potential evaporation ( $\sigma_{E_p}$ ). Most of previous studies that examined the interannual variability of precipitation and potential evaporation focused on their impact on the interannual variability of evapotranspiration [31,32], following the work of Koster and Suarez [30]. It is however less clear how the interannual variability of precipitation and potential evaporation would affect the long-term mean annual evapotranspiration.

Assessing the impact of interannual variability of precipitation and potential evaporation on the long-term mean annual evapotranspiration can help understand departures of observational data from the Budyko curve as reported by many previous studies. Many factors have been documented to potentially cause departures from the Budyko curve, including land surface characteristics such as vegetation [21,33–35], topography [36], soil properties [37,38], and human activities [28,39]. A few studies have examined the seasonal variability of precipitation and potential evaporation within the Budyko framework. For example, Budyko and Zubenok [40] noted that the evaporation ratio ( $E/P$ ) tends to be higher in climates where precipitation and potential evaporation are in phase and lower where they are out of phase. This has been theoretically justified by Milly [41] and Feng et al. [42] using dimensional analysis and stochastic soil moisture models, as well as by Yokoo et al. [38] using a physically-based water balance model. However, the opposite is found by Potter et al. [43] using data from 262 catchments in Australia; that is, the catchments where precipitation and potential evaporation is in phase have lower evaporation ratios

than those catchments where precipitation and potential evaporation is out of phase. They attributed this discrepancy between results from a stochastic soil moisture model and observations to the infiltration-excess runoff that is not explicitly considered in the stochastic soil moisture model. The interannual variability of precipitation and potential evaporation, on the other hand, has received much less attention, which motivates this study.

To examine how changes in the interannual variability of precipitation and potential evaporation would affect the long-term mean annual evapotranspiration as well as the interannual variability of evapotranspiration, a stochastic soil moisture model is employed (the model details are given in Rodríguez-Iturbe and Porporato [1]). A simple stochastic soil moisture model, instead of observational data sets or climate model results, is used to study this problem because it is difficult to identify changes in the interannual variability of precipitation and potential evaporation at a given location due to temporal limitations in the data [44]. It is also challenging to separate the effect of interannual variability of precipitation and potential evaporation from the effects of other factors such as land cover change using climate models given the complexities of these models [45]. In addition, it is difficult, if not impossible, to conduct sensitivity analysis based on observational datasets or global/regional climate models. As such, theoretical analyses and numerical simulations based on a simple and computationally cheap stochastic soil moisture model like the one used in this study can be particularly useful for unraveling the hydroclimatic impacts of interannual variability of precipitation and potential evaporation.

The paper is organized as follows: Section 2 describes the stochastic soil moisture model and the methodology; Section 3

discusses the results and Section 4 presents the conclusions and discusses the implications of this study.

## 2. Methodology

### 2.1. The stochastic soil moisture model

The details of the stochastic soil moisture model has been described in Laio et al. [46] and Rodríguez-Iturbe and Porporato [1]. Here only the essence of the model is presented. The model starts with the vertically-averaged soil water balance (Eq. (1)) at a given point where lateral contributions to the soil water balance can be neglected:

$$nZ_r \frac{ds}{dt} = P(t) - I(t) - Q(s, t) - E(s) - L(s), \quad (1)$$

where  $n$  is the soil porosity,  $Z_r$  is the root zone depth,  $s$  is the relative soil moisture,  $t$  is time,  $P(t)$  is the rainfall rate,  $I(t)$  is the interception of rainfall by canopy,  $Q(s, t)$  is the runoff,  $E(s)$  is the evapotranspiration rate and  $L(s)$  is the leakage rate. Following Rodríguez-Iturbe and Porporato [1], the stochasticity in the soil moisture dynamics primarily comes from the stochastic nature of rainfall and the model is interpreted as a continuous model at daily scales. At such temporal scales, rainfall is modeled as a stochastic, marked Poisson process: the times between daily rainfall events follows a Poisson distribution with mean  $1/\lambda$  and the daily rainfall depth follows an exponential distribution with mean  $\alpha$ .

The interception of rainfall is modeled by assuming that rainfall depth that is below a fixed threshold  $\Delta$  is intercepted (i.e., when the daily rainfall depth is less than  $\Delta$ , no rain water will reach the ground surface). When the rain water reaches the ground surface, infiltration and runoff occur. If the rainfall depth (after interception) is smaller than the available storage, all rain water infiltrates into the subsurface. On the other hand, if the rainfall depth is larger than the available storage, the available storage will be filled up first and the excess is converted into runoff subsequently.

The evapotranspiration is modeled as:

$$E(s) = \begin{cases} 0 & 0 < s \leq s_h \\ E_w \frac{s-s_h}{s_w-s_h} & s_h < s \leq s_w \\ E_w + (E_p - E_w) \frac{s-s_w}{s^*-s_w} & s_w < s \leq s^* \\ E_p & s^* < s \leq 1 \end{cases} \quad (2)$$

where  $E_w$  is the evapotranspiration rate when the soil moisture is at the wilting point ( $s_w$ ) and  $E_p$  is the potential evaporation rate when soil moisture is sufficient (i.e., above a certain point  $s^*$  in this case).  $s_h$  is the hygroscopic point below which evapotranspiration is modeled as zero. The leakage loss is modeled as if it happens only when the soil moisture is above the field capacity ( $s_{fc}$ ):

$$L(s) = \begin{cases} 0 & s \leq s_{fc} \\ \frac{K_s}{e^{\beta(1-s_{fc})}-1} [e^{\beta(s-s_{fc})} - 1] & s_{fc} < s \leq 1 \end{cases} \quad (3)$$

where  $K_s$  is the saturated hydraulic conductivity and  $\beta$  is a coefficient that depends on the soil–water retention curve.

Given all of these models for different components of the soil water balance, a steady-state probability density function (*pdf*) can be obtained for soil moisture, as follows:

$$p(s) = \begin{cases} \frac{C}{\eta_w} \left( \frac{s-s_h}{s_w-s_h} \right)^{\lambda' \frac{s_w-s_h}{\eta_w}} e^{-\gamma s} & s_h < s \leq s_w \\ \frac{C}{\eta_w} \left[ 1 + \left( \frac{\eta}{\eta_w} - 1 \right) \left( \frac{s-s_w}{s^*-s_w} \right) \right]^{\lambda' \frac{s^*-s_w}{\eta_w}-1} e^{-\gamma s} & s_w < s \leq s^* \\ \frac{C}{\eta} e^{-\gamma s + \frac{\lambda'}{\eta}(s-s^*)} \left( \frac{\eta}{\eta_w} \right)^{\lambda' \frac{s^*-s_w}{\eta_w}} & s^* < s \leq s_{fc} \\ \frac{C}{\eta} e^{-(\beta+\gamma)s + \beta s_{fc}} \left( \frac{\eta e^{\beta s}}{(\eta-m)e^{\beta s_{fc}} + m e^{\beta s}} \right)^{\frac{\lambda'}{\beta(\eta-m)}+1} \left( \frac{\eta}{\eta_w} \right)^{\lambda' \frac{s^*-s_w}{\eta_w}} e^{\frac{\lambda'}{\eta}(s_{fc}-s^*)} & s_{fc} < s \leq 1 \end{cases} \quad (4)$$

where  $C$  is a constant that can be obtained through evaluating  $\int_0^1 p(s)ds = 1$ .  $\eta_w = E_w/(nZ_r)$  and  $\eta = E_p/(nZ_r)$  are normalized wilting point evaporation and potential evaporation, respectively.  $m = K_s/[nZ_r(e^{\beta(1-s_{fc})} - 1)]$  is a “normalized” saturated hydraulic conductivity.  $\gamma = \alpha/(nZ_r)$  and  $\lambda' = \lambda e^{-\Delta/\alpha}$  are related to rainfall characteristics, that is, the daily rainfall depth ( $\alpha$ ) and the frequency of daily rainfall events ( $\lambda$ ). Note when  $\Delta = 0$  (i.e., no interception occurs),  $\lambda' = \lambda$ .

The average soil moisture and evapotranspiration resulting from the stochastic model presented above are calculated following:

$$\langle s \rangle = \int_0^1 s p(s) ds, \quad (5)$$

$$\langle E \rangle = \int_0^1 E(s) p(s) ds = \int_{s_h}^1 E(s) p(s) ds, \quad (6)$$

and the average rainfall that reaches the ground surface is calculated as:

$$\langle P \rangle = \alpha \lambda'. \quad (7)$$

This stochastic soil moisture model has been validated by field experiments. For example, Salvucci [47] estimated the soil water loss function (Eq. (2) + Eq. (3)) from observational data at various sites in Illinois, USA and then calculated the soil moisture *pdf*, given estimates of  $\alpha$  and  $\lambda$  at the same locations. The calculated *pdf* of soil moisture is in good agreement with the measurements (see the Fig. 4 in Salvucci [47]).

### 2.2. Numerical experiments design

Since the focus of this study is to understand the impact of interannual precipitation and potential evaporation variability on the long-term mean annual evapotranspiration, parameters other than the rainfall characteristics (i.e.,  $\alpha$  and  $\lambda$ ) and potential evaporation ( $E_p$ ) are not changed. Their values are adopted from Rodríguez-Iturbe and Porporato [1] and are listed in the Table 1. The soil is assumed to be loamy sand and the value of  $E_w$  is typically found in the literature [46]. The interception threshold ( $\Delta$ ) is set to be zero in order to simplify the analysis. Note that the effect of increasing the interception threshold on the evaporation ratio is equivalent to that of reducing the parameter  $\lambda$  since  $\lambda' = \lambda e^{-\Delta/\alpha}$  is the parameter needed in Eqs. (4) and (7). Given that  $\Delta/\alpha$  is usually small at interannual scales, changes in  $\Delta$  are not likely to result in significant changes in the  $\lambda$ . The root zone depth ( $Z_r$ ) is chosen to be 30 cm and the sensitivity to the root zone depth is also analyzed later. The value of  $E_p$  listed in Table 1 is the long-term mean annual potential evaporation [46]. As shall be seen later, the annual potential evaporation will be different from this value for some simulations.

**Table 1**  
Parameters used in the stochastic soil moisture model.

Variables	Values
$s_h$	0.08
$s_w$	0.11
$s^*$	0.31
$s_{fc}$	0.52
$n$	0.42
$\beta$	12.7
$K_s$ (cm/day)	100
$E_w$ (cm/day)	0.01
$E_p$ (cm/day)	0.45
$\Delta$	0
$Z_r$ (cm)	30

In order to assess the impact of interannual variability of precipitation and potential evaporation, Monte Carlo simulations are conducted in order to numerically estimate the long-term mean annual evapotranspiration resulting from random fluctuations of  $\alpha$ ,  $\lambda$  and  $E_p$ . Previous studies have analyzed long-record rainfall data and found that  $\alpha$  and  $\lambda$  follow gamma distributions closely at inter-annual time scales [48]. Annual potential evaporation is assumed to follow a Gaussian distribution [49]. Gamma distribution and Gaussian distribution are both two-parameter distributions and hence a mean value and a coefficient of variation (CV, defined as the standard deviation normalized by the mean) value are needed to specify the distribution. The long-term mean values of  $\alpha$  and  $\lambda$  are randomly sampled for 500 times within the ranges from 0.1 to 2.5 cm (interval = 0.049 cm) and from 0.1 to 0.5 day<sup>-1</sup> (interval = 0.0082 day<sup>-1</sup>), respectively. The long-term mean value of  $E_p$  is 0.45 cm/day as listed in Table 1. Through this procedure, the sampled long-term mean values of  $\alpha$  and  $\lambda$  and the concomitant dryness index ( $E_p/P$ ) cover a wide range of climates.

Given the long-term mean of  $\alpha$ ,  $\lambda$  and  $E_p$ , twenty sets of simulations with different CV values are conducted, as shown in Table 2. For each year, an array of ( $\alpha$ ,  $\lambda$ ,  $E_p$ ) is randomly sampled from their respective distributions and the resulting average (i.e., annual) soil moisture  $\langle s \rangle$ , average evapotranspiration  $\langle E \rangle$ , and average rainfall  $\langle P \rangle$  are calculated from Eqs. (5)–(7), respectively. As can be seen from Table 2, the cases 1–4 are designed to investigate the impact of inclusion of the interannual variability of rainfall in the stochastic soil moisture model. In case 1, the daily rainfall depth  $\alpha$  and the frequency of daily rainfall events  $\lambda$  are set to be constant. As such, there is no interannual variability of  $\alpha$  and  $\lambda$ . The annual values of  $\alpha$  and  $\lambda$  are identical to their long-term mean values, respectively. In case 2, the daily rainfall depth  $\alpha$  is set to be constant over the time period, while the frequency of daily rainfall events  $\lambda$  is randomly sampled from a gamma distribution whose mean value is identical to that in case 1 and whose coefficient of variation is set to be 0.21. As such, the long-term mean annual precipitation remains identical to that in case 1 if the sample size is sufficiently large (in this study, 300 is chosen to represent a 300-year period); and the difference between the two cases lies in the interannual variability of precipitation. Similarly, in case 3, the frequency of daily rainfall events  $\lambda$  is set to be constant over the time period, while the daily

rainfall depth  $\alpha$  is randomly sampled from a gamma distribution whose mean value is identical to that in case 1 and whose CV is set to be 0.35. In case 4, both  $\alpha$  and  $\lambda$  are randomly sampled from their respective gamma distributions. It is again stressed that the long-term mean annual precipitation of the four cases are extremely close due to the large sample size used in this study. The difference among the four cases is only the interannual variability of precipitation.

In cases 5–8, the interannual variability of daily rainfall depth ( $\alpha$ ) is included but the interannual variability of the frequency of daily rainfall events ( $\lambda$ ) is excluded; while in cases 9–12, the interannual variability of the frequency of daily rainfall events ( $\lambda$ ) is included but the interannual variability of daily rainfall depth ( $\alpha$ ) is not. When the interannual variability of daily rainfall depth ( $\alpha$ ) is considered, the CV values of  $\alpha$  vary from 0.15 to 0.45, with an interval of 0.1. When the interannual variability of the frequency of daily rainfall events ( $\lambda$ ) is considered, the CV values of  $\lambda$  vary from 0.11 to 0.41, with an interval of 0.1. Again, the long-term mean annual precipitation of these cases remains similar. The last eight sets of simulations are designed to study the interannual variability of potential evaporation. The potential evaporation in cases 13–16 has a CV value of 0.22 and the CV values of  $\alpha$  and  $\lambda$  are identical to those in cases 1 to 4, respectively. In cases 17–20, only the interannual variability of potential evaporation is retained and the potential evaporation increases its CV value from 0.12 to 0.42 with an interval of 0.1.

The CV values of  $\alpha$ ,  $\lambda$  and  $E_p$  are all in broad consistency with the values reported the literature. For example, the CV of  $\alpha$  obtained by Porporato et al. [50] over the Kalahari transect ranges from 0.16 to 0.31 and the CV of  $\lambda$  ranges from 0.12 to 0.32. The CV of  $\alpha$  reported by D'Odorico et al. [48] over southern Texas ranges from 0.26 to 0.45 and the CV of  $\lambda$  ranges from 0.19 to 0.27. Ridolfi et al. [51] analyzed the impact of interannual variability of precipitation on the soil moisture dynamics using Monte Carlo simulations. The CV of  $\alpha$  used in Ridolfi et al. [51] ranges from 0 to 0.3 and the CV of  $\lambda$  ranges from 0 to 0.4. Daly and Porporato [49] examined the daily variability of  $E_p$  and reported a CV value of 0.54, which provides an upper bound for the CV of  $E_p$  at interannual scales. In addition, the interannual variability of  $E_p$  estimated by Arora [52] translates to a CV value of about 0.05–0.4.

### 2.3. The Budyko curve

As discussed in the introduction, the Budyko curve is widely used to analyze the long-term, basin-scale water and energy balances due to its simplicity and universality. In the Budyko framework, the evaporation ratio ( $E/P$ ) is only a function of the dryness index ( $E_p/P$ ) at long-term scales. The Budyko curve expressed by Fu's equation [20] is as follows:

$$\frac{E}{P} = f\left(\frac{E_p}{P}\right) = 1 + \frac{E_p}{P} - \left[1 + \left(\frac{E_p}{P}\right)^\varpi\right]^{1/\varpi}, \quad (8)$$

where  $\varpi$  is a shape parameter that reflects the impact of all other factors such as land surface characteristics and climate fluctuations on evapotranspiration. When  $\varpi = 2.6$ , the above equation recovers the very original Budyko curve proposed by Budyko himself [53,54].

Koster and Suarez [30] derived an analytical expression for the interannual variability of evapotranspiration ( $\sigma_E$ ) based on the Budyko curve but at annual scales. The full expression for  $\sigma_E$  is:

$$\left(\frac{\sigma_E}{\sigma_P}\right)^2 = \left[f\left(\frac{E_p}{P}\right) - \frac{E_p}{P}f'\left(\frac{E_p}{P}\right)\right]^2 + \left[f'\left(\frac{E_p}{P}\right)\frac{\sigma_{E_p}}{\sigma_P}\right]^2. \quad (9)$$

where  $f$  is the function in Eq. (8) and  $f'$  is the derivative of  $f$ . Note the above equation also assumes that there is no correlation between annual precipitation and annual potential evaporation, which may

**Table 2**

Interannual variability of precipitation and potential evaporation included in different sets of simulations.

Number	CV [ $\alpha$ ]	CV [ $\lambda$ ]	CV [ $E_p$ ]
1	0	0	0
2	0	0.21	0
3	0.35	0	0
4	0.35	0.21	0
5	0.15	0	0
6	0.25	0	0
7	0.35	0	0
8	0.45	0	0
9	0	0.11	0
10	0	0.21	0
11	0	0.31	0
12	0	0.41	0
13	0	0	0.22
14	0	0.21	0.22
15	0.35	0	0.22
16	0.35	0.21	0.22
17	0	0	0.12
18 <sup>a</sup>	0	0	0.22
19	0	0	0.32
20	0	0	0.42

<sup>a</sup> Case 18 is identical to case 13. It is however listed separately from case 13 so that the last four cases in Table 2 appears to be dedicated for examining the increasing interannual variability of potential evaporation

not be the case for some basins [55]. Further assuming that the interannual variability of potential evaporation ( $\sigma_{Ep}$ ) is small compared to the interannual variability of precipitation ( $\sigma_P$ ), Eq. (9) can be reduced to:

$$\frac{\sigma_E}{\sigma_P} = f\left(\frac{E_p}{P}\right) - \frac{E_p}{P} f'\left(\frac{E_p}{P}\right). \quad (10)$$

### 3. Results

#### 3.1. The impact of interannual variability of precipitation on the long-term mean annual evapotranspiration

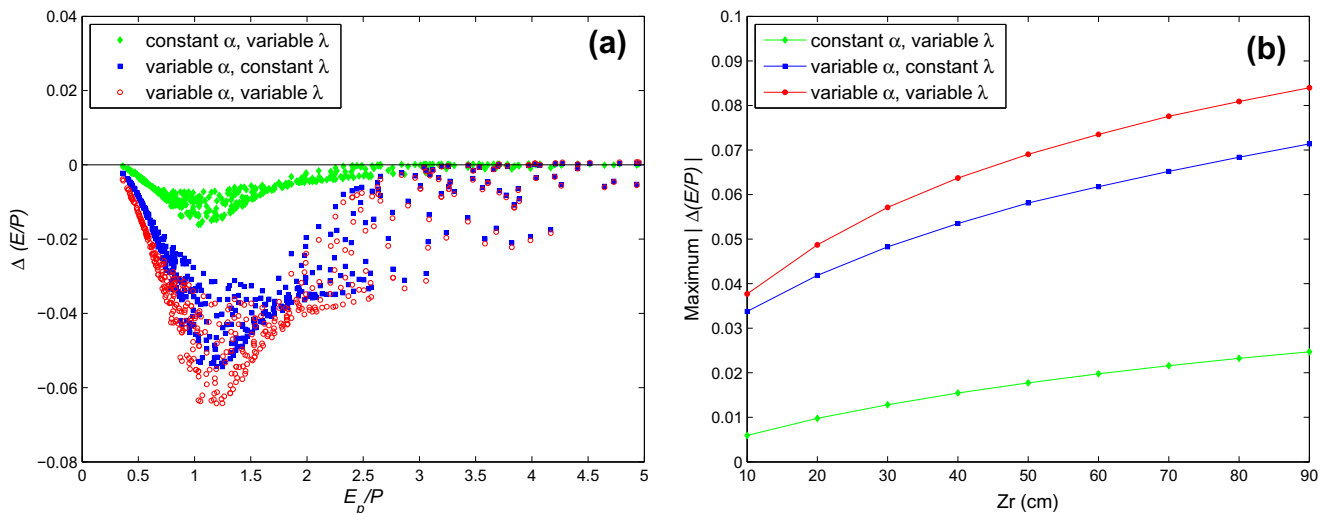
The long-term mean annual evaporation ratios calculated from cases 1 to 4 are inter-compared, as shown in Fig. 1. The Budyko curve is from Fu's equation (Eq. (8)) with  $\varpi$  obtained from fitting Fu's equation to the data (see Li et al. [54] for the fitting procedure). When the interannual variability of precipitation is not included (i.e.,  $\alpha$  and  $\lambda$  are both constants over the 300-year time period), the resulting long-term water and energy balances from the stochastic model follow a Budyko curve with  $\varpi = 3.5$  (Fig. 1(a)). As the interannual variability of rainfall is included (i.e.,  $\alpha$  and/or  $\lambda$  both vary over the 300-year time period), the long-term evaporation ratios are reduced as reflected by the smaller  $\varpi$  values (Fig. 1(b)–(d)).

Using case 1 as a reference, Fig. 2 examines the differences in the long-term mean annual evaporation ratios in cases 2–4. As can be seen from Fig. 2(a), the impact of varying  $\alpha$  and/or  $\lambda$  on the long-term mean annual evaporation ratios is most prominent when the dryness index is within the range from 0.5 to 2. Note for these four cases, the long-term mean annual precipitation remains similar and the long-term mean annual potential evaporation is identical. As such, the reductions shown in Fig. 2(a) are solely induced by the interannual variability of precipitation. When  $\alpha$  and  $\lambda$  both vary, the maximum reduction in the long-term mean annual evaporation ratios reaches 7%, which occurs at the dryness index of about 1.25. It is interesting to observe that the long-term mean annual evaporation ratios are more sensitive to  $\alpha$  than  $\lambda$  (cf. the blue and green dots in Fig. 2(a)). As shall be seen later, this is related to the different CV values of  $\alpha$  and  $\lambda$  as well as the different effects of  $\alpha$  and  $\lambda$  on the pdf of soil moisture (Eq. (4)). Note the CV values of  $\alpha$  and  $\lambda$  used here are typical values

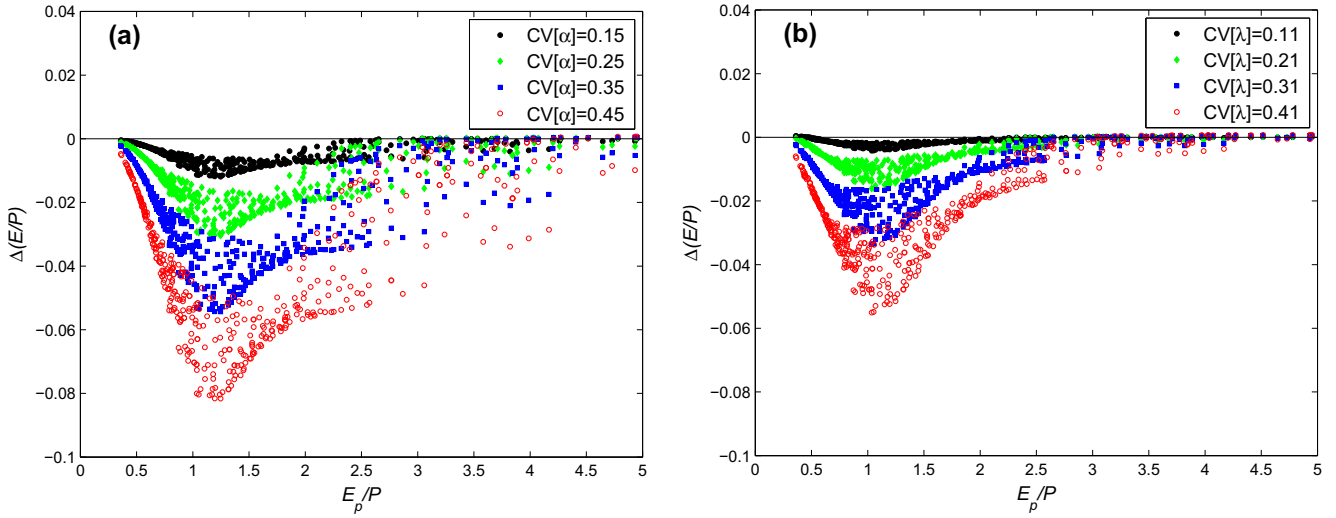
reported by D'Odorico et al. [48] based on rainfall data in southern Texas. In the following, a range of CV values of  $\alpha$  and  $\lambda$  will be used.

Fig. 2(b) examines the reductions in the evaporation ratio as the root zone depth ( $Z_r$ ) changes. For a wide range of possible values of  $Z_r$ , only reductions in the evaporation ratio are observed when the interannual variability of precipitation is included. Given the scatter observed in Fig. 2(a) around the maximum reduction, the maximum reductions shown in Fig. 2(b) are calculated as the mean of those data exceeding the 90th percentile. It is clear that the maximum reductions in the evaporation ratio increase as the root zone depth ( $Z_r$ ) increases. This is because the evaporation ratio is higher for deep-rooted soils and hence the effect of increasing precipitation variability on the evaporation ratio is also enhanced. This finding is consistent with the study of Daly and Porporato [49], which showed that under the same climatic conditions, evapotranspiration is reduced when the daily variability of potential evaporation is considered and this reduction effect is larger for deep-rooted soils than for shallow-rooted soils.

In order to assess the effect of  $\alpha$  (daily rainfall depth) and  $\lambda$  (frequency of daily rainfall events) separately, Fig. 3 shows the differences in the long-term mean annual evaporation ratios when one parameter is kept constant while the other parameter increases its CV value. Fig. 3(a) keeps the frequency of daily rainfall events  $\lambda$  constant with the CV of  $\alpha$  increasing from 0.15 to 0.45; while Fig. 3(b) keeps the daily rainfall depth  $\alpha$  constant with the CV of  $\lambda$  increasing from 0.11 to 0.41. It is clear that varying either of the two parameters reduces the long-term mean annual evaporation ratios. For all cases, the reductions are mostly prominent when  $E_p/P$  is within the range from 0.5 to 2, which is in agreement with Fig. 2. It is also clear that as the variability (i.e., the CV value) increases, the reductions in the long-term mean annual evaporation ratios increase. Fig. 4 shows the maximum reductions in the long-term mean annual evaporation ratios as a function of the CV values of  $\alpha$  and  $\lambda$ . In addition, in order to reveal the 'true' relation between the maximum reductions and the CV values of  $\alpha$  and  $\lambda$ , more simulations are conducted. For example, when the interannual variability of  $\alpha$  is considered, simulations with CV values of 0.1, 0.2, 0.3 and 0.4 are added. Similarly, when the interannual variability of  $\lambda$  is considered, simulations with CV values of 0.16, 0.26, 0.36 and 0.46 are added. As can be seen, the relations between the maximum reductions in the long-term mean annual evaporation ratios and the CV values of  $\alpha$  and  $\lambda$  can be adequately described by power laws with  $R^2 = 0.999$  and  $p < 0.001$  (from  $t$ -test).



**Fig. 2.** (a) Differences in the long-term mean annual evaporation ratios ( $\Delta E/P = (E/P)_{2,3,4} - (E/P)_1$ ); (b) maximum differences in the long-term mean annual evaporation ratios ( $\Delta E/P = (E/P)_{2,3,4} - (E/P)_1$ ) as a function of root zone depth ( $Z_r$ ).



**Fig. 3.** Differences in the long-term mean annual evaporation ratios ( $\Delta(E/P) = (E/P)_x - (E/P)_1$ ). The subscript  $x$  denotes cases 5–8 in (a) and 9–12 in (b).

Comparing Fig. 4(a) and (b) reveals that even with the same CV value, the maximum reductions in evaporation ratio resulting from including variability of  $\alpha$  or  $\lambda$  are different. This is due to the different roles of  $\alpha$  or  $\lambda$  in affecting the pdf of soil moisture (Eq. (4)) and hence the evapotranspiration (Eq. (6)). For example, Porporato et al. [56] used a minimalist approach to solve the soil water balance equation and found that the shape of the resulting Budyko curve (see Fig. 1), which is described by  $\varpi$  in Eq. (8), is determined by the ratio  $w_o/\alpha$ , where  $w_o = nZr(s_{fc} - s_w)$  is the maximum soil water storage available to plants (see Cong et al. [57] and Yang et al. [58] for the relationship between  $\varpi$  and  $w_o/\alpha$ ). Hence  $\lambda$  does not affect the shape of the Budyko curve.

It is also interesting to observe that the dryness index at which the maximum reductions occur does not change with the CV values of  $\alpha$  and  $\lambda$  (not shown here but can be inferred from Fig. 3); that is, the dryness index at which the maximum reductions occur is always about 1.25. This is simply due to the use of gamma distributions for  $\alpha$  and  $\lambda$ . When Gaussian distributions with identical mean and CV values are used instead, the dryness index at which the maximum reductions occur changes with the CV values of  $\alpha$  and  $\lambda$  (not shown). This will be seen in Section 3.2 where potential evaporation is assumed to follow a Gaussian distribution.

### 3.2. The impact of interannual variability of potential evaporation on the long-term mean annual evapotranspiration

The previous section examined the impact of the interannual variability of precipitation, including the interannual variability of daily rainfall depth and the interannual variability of frequency of daily rainfall events, on the long-term mean annual evapotranspiration. This section studies the impact of interannual variability of potential evaporation on the long-term mean annual evapotranspiration. Following Daly and Porporato [49], when the interannual variability of potential evaporation is considered, the annual potential evaporation is assumed to follow a Gaussian distribution. Fig. 5(a) shows the differences in the long-term annual evaporation ratios between cases considering the interannual variability of  $E_p$  (cases 13–16) and cases without considering the interannual variability of  $E_p$  (cases 1–4). As can be seen, including the interannual variability of  $E_p$  also reduces the long-term mean annual evaporation ratios. It is interesting to observe that whether including the interannual variability of  $P$  or not has little impact on the reductions induced by including the interannual variability of  $E_p$ , implying that there is no interaction between the interannual variability of  $P$  and  $E_p$  and hence their impacts on the long-term

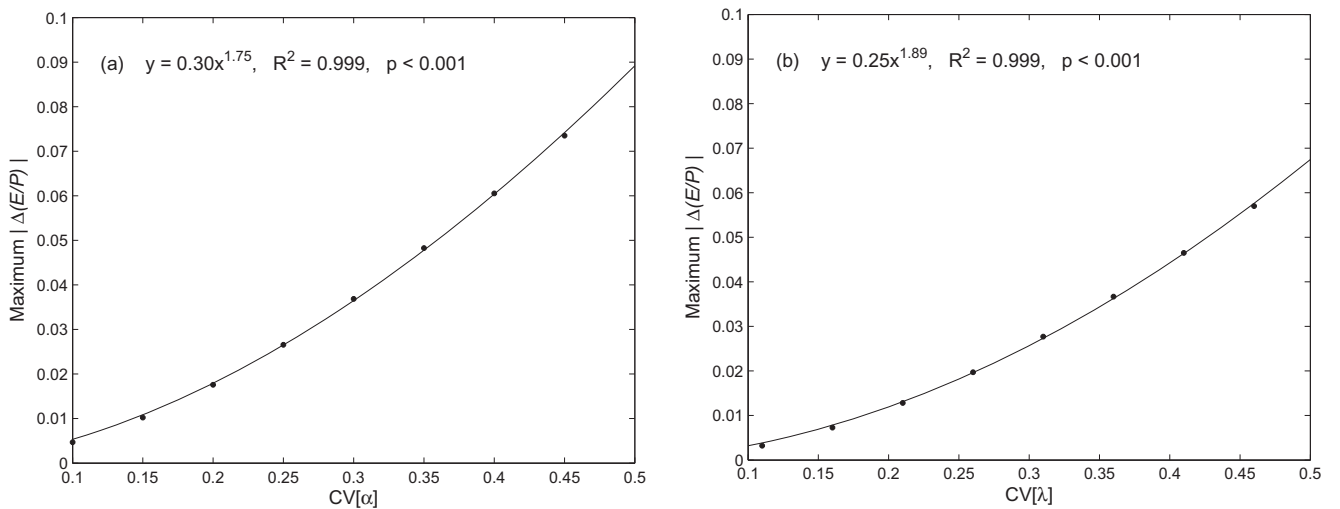


**Fig. 4.** Maximum reductions in the long-term mean annual evaporation ratios as a function of CV values of (a)  $\alpha$  and (b)  $\lambda$ .

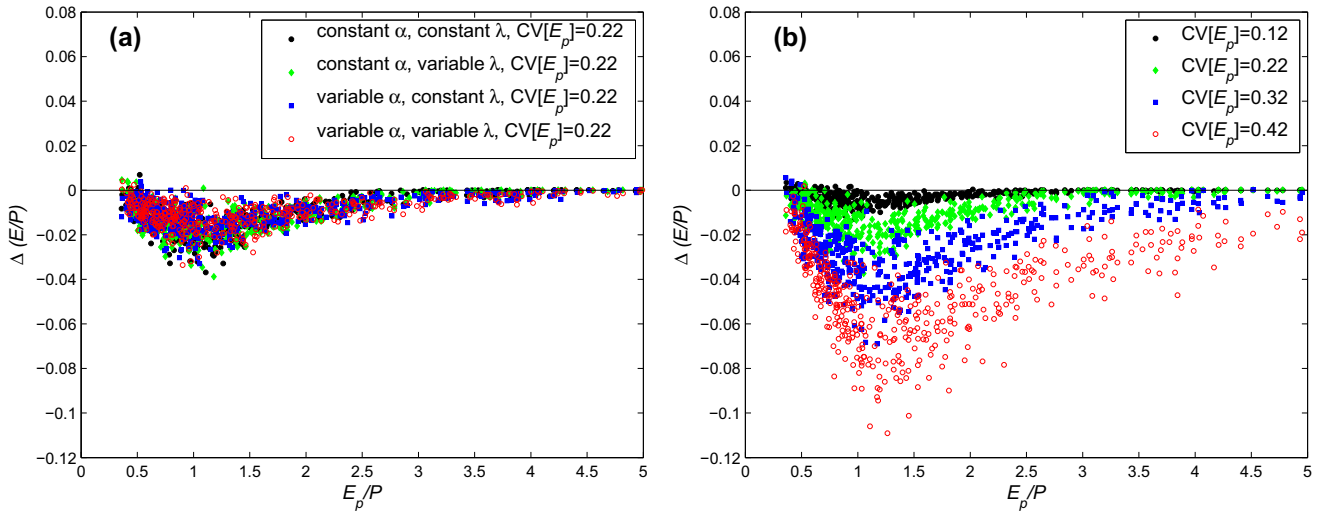


**Fig. 5.** Differences in the long-term mean annual evaporation ratios for examining the impact of the interannual variability of potential evaporation. (a) Shows the differences between cases 13–16 and cases 1–4, respectively; (b) shows the differences between cases 17–20 and case 1.

mean annual evapotranspiration can be additive. Fig. 5(b) shows that reductions in the long-term annual evaporation ratios increase as the interannual variability of  $E_p$  increases. When the maximum reductions in the long-term annual evaporation ratios are concerned, it is shown in Fig. 6(a) that the relation between maximum reductions in the long-term annual evaporation ratios and the CV value of  $E_p$  also satisfies a power law. This is similar to the observation in Fig. 4. However, unlike that the interannual variability of precipitation does not affect the dryness index at which the maximum reductions occur, the interannual variability of  $E_p$  does alter this dryness index: The dryness index at which the maximum reductions occur increases with the CV value of  $E_p$ , as shown in Fig. 6(b). As discussed in Section 3.1, this is caused by the use of a Gaussian distribution for  $E_p$  instead of a gamma distribution.

Daly and Porporato [49] examined the impact of including daily variability of  $E_p$  on soil moisture dynamics. The temporal fluctuations in  $E_p$  are assumed to be Gaussian and the resulting soil water balance equation (Eq. (1)) is a stochastic differential equation forced by a Poisson noise (representing precipitation fluctuations) and a multiplicative Gaussian white noise (representing potential evaporation fluctuations). By analytically solving this stochastic

differential equation, they also found that including the daily variability of  $E_p$  reduces evapotranspiration, which is in agreement with the results presented in this study, albeit at different time scales.

### 3.3. The impact of interannual variability of precipitation and potential evaporation on the interannual variability of evapotranspiration

In this section, the impact of interannual variability of precipitation and potential evaporation on the interannual variability of evapotranspiration is investigated. As discussed in the introduction, Koster and Suarez [30] provided a simple framework to examine the interannual variability of evapotranspiration. According to Eq. (10), the ratios of interannual variability of evapotranspiration and interannual variability of rainfall ( $\sigma_E/\sigma_P$ ) follow a semi-empirical curve that is only a function of the dryness index ( $E_p/P$ ) if the interannual variability of potential evaporation and the correlation between precipitation and potential evaporation are assumed to be small. As can be seen from Fig. 7(a), the interannual variability of evapotranspiration generated from the stochastic soil moisture model follows the semi-empirical curve proposed by Koster and

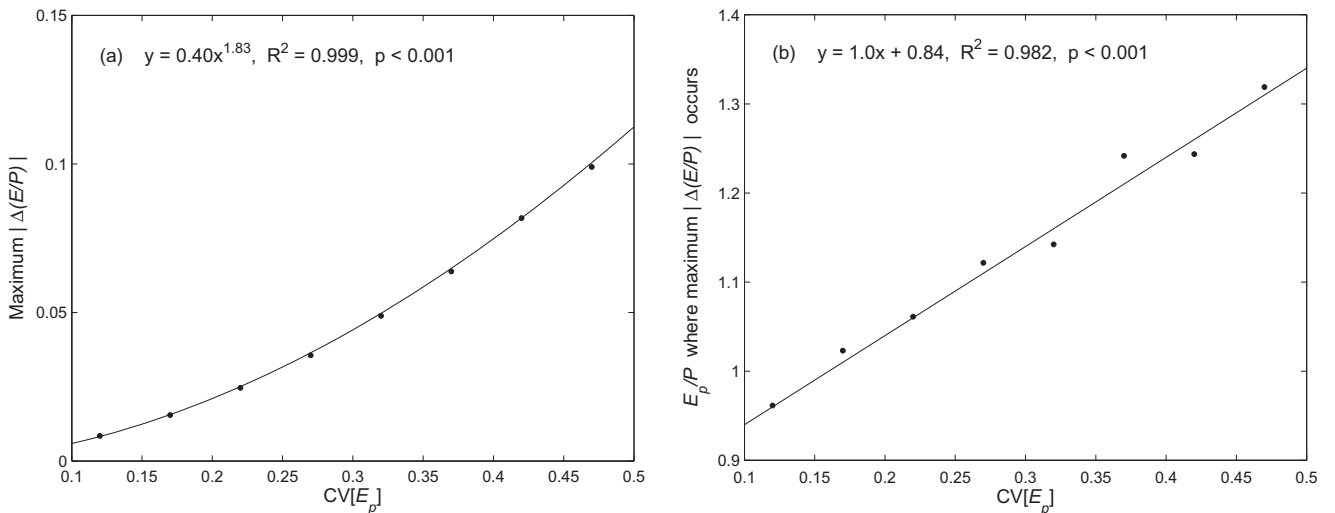


**Fig. 6.** (a) Maximum reductions in the long-term mean annual evaporation ratios as a function of CV values of  $E_p$ ; (b) the dryness index at which the maximum reductions in the long-term mean annual evaporation ratios occur as a function of CV values of  $E_p$ .

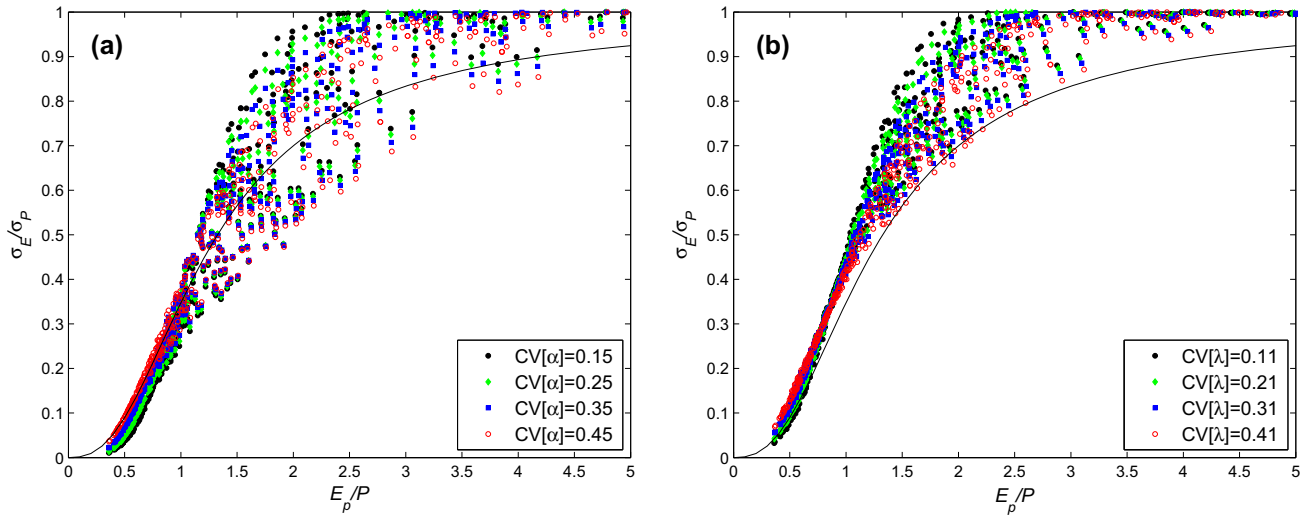


**Fig. 7.** The ratios of interannual variability of evapotranspiration and rainfall ( $\sigma_E/\sigma_P$ ) are shown as a function of the long-term mean annual dryness index ( $E_p/P$ ). (a) Shows cases when the daily rainfall depth is variable (cases 5–8 in Table 2); while (b) shows cases when the frequency of daily rainfall events is variable (cases 9–12 in Table 2). The black line is given by Koster and Suarez [30] (see Eq. (10)) with Fu's equation used for describing the Budyko curve.

Suarez [30] fairly well when only the interannual variability of daily rainfall depth ( $\alpha$ ) is considered (cases 5–8). Nevertheless, when only the interannual variability of the frequency of daily rainfall events ( $\lambda$ ) is considered (cases 9–12), the resulting  $\sigma_E/\sigma_P$  deviates from the semi-empirical curve proposed by Koster and Suarez [30], especially under dry conditions (see Fig. 7(b) when the dryness index  $>1$ ). Note that a range of CV values are used for considering the interannual variability of  $\lambda$ . The fact that all the resulting data do not agree with the empirical curve proposed by Koster and Suarez [30] under dry conditions clearly suggests that one cannot reproduce the empirical curve proposed by Koster and Suarez [30] without considering the interannual variability of  $\alpha$ . Using the empirical curve proposed by Koster and Suarez [30] as a reference, this suggests that the interannual variability of daily rainfall depth ( $\alpha$ ) and frequency of daily rainfall events ( $\lambda$ ) have quantitatively different impacts on the interannual variability of evapotranspiration. When both interannual variability are considered, the agreement between the simulated results and the semi-empirical curve proposed by Koster and Suarez [30] is excellent (not shown). This implies that the interannual variability of evapotranspiration is mostly controlled by the interannual variability of precipitation and the dryness index, which suggests that the effect of interannual water storage change is probably insignificant and hence it is reasonable to use the steady-state soil moisture pdf (i.e., Eq. (4)).

Fig. 7 also shows that under dry conditions, the scatter is much larger than that under wet conditions, suggesting that the ratio  $\sigma_E/\sigma_P$  is no longer solely dependent on the dryness index. Given that the long-term mean annual potential evaporation is constant for these cases, the large scatter seen in Fig. 7 under dry conditions implies that  $\sigma_E/\sigma_P$  can be different when the long-term mean annual precipitation is the same. Since the CV value is specified for each case, it further indicates that the ratio  $\sigma_E/\sigma_P$  can be different even when the interannual variability of precipitation ( $\sigma_P$ ) is identical; that is, the different rainfall generation processes can produce different  $\sigma_E/\sigma_P$  ratios. This effect is more prominent under dry conditions because evapotranspiration is controlled by water availability under such conditions. It is also interesting to observe that under dry conditions, increasing the CV of  $\alpha$  and  $\lambda$  nevertheless results in decreases in  $\sigma_E/\sigma_P$ , which is due to the fact that the resulting increase in  $\sigma_P$  is faster than the increase in  $\sigma_E$  under such conditions. Under wet conditions (when the dryness index

$<1$ ), increasing the CV values of  $\alpha$  and  $\lambda$  however results in increases in  $\sigma_E/\sigma_P$ , which is caused by increases in  $\sigma_E$ .

The Eq. (10) assumes that the interannual variability of potential evaporation is small as compared to the interannual variability of precipitation. When this is not the case, deviations from Eq. (10) are expected and Eq. (9) is needed to describe the relationship between the interannual variability of evapotranspiration, precipitation and potential evaporation. As shown in Fig. 8, cases with variable  $E_p$  (cases 14–16, circles on Fig. 8) are clearly different from cases with constant  $E_p$  (cases 2–4, dots on Fig. 8). Including the interannual variability of potential evaporation mostly affects the interannual variability of evapotranspiration when the dryness index is smaller than 1, that is, under wet conditions. This is because evapotranspiration is controlled by energy availability and hence potential evaporation under such condition. It can be also inferred from Eq. (9) since  $f$  increases with decreasing dryness index. As such, the second term of the right hand side of Eq. (9) (or the impact of interannual variability of potential evaporation)

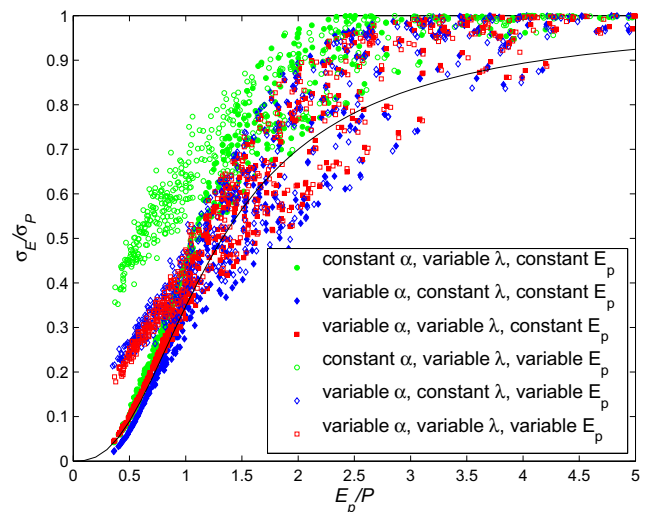


**Fig. 8.** The ratios of interannual variability of evapotranspiration and rainfall ( $\sigma_E/\sigma_P$ ) are shown as a function of the long-term mean annual dryness index ( $E_p/P$ ) for cases 2–4 and 14–16 in Table 2. The black line is given by Koster and Suarez [30] (see Eq. (10)) with Fu's equation used for describing the Budyko curve.

increases as the dryness index decreases. It is however pointed out that the impact of interannual variability of potential evaporation is different when the interannual variability of daily rainfall depth ( $\alpha$ ) and that of the frequency of daily rainfall events ( $\lambda$ ) are included differently, which cannot be inferred from Eq. (9). Keeping the daily rainfall depth constant clearly enhances the interannual variability of evapotranspiration, as compared to results when the daily rainfall depth varies (c.f. the green circles and the blue/red circles). When the daily rainfall depth is variable, varying the frequency of daily rainfall events ( $\lambda$ ) shows little effect on the resulting  $\sigma_E/\sigma_P$  (c.f. the blue and the red circles). Figs. 7 and 8 suggest that the interannual variability of daily rainfall depth ( $\alpha$ ) and that of the frequency of daily rainfall events ( $\lambda$ ) play different roles in modulating the interannual variability of evapotranspiration. They also interact differently with the interannual variability of potential evaporation.

#### 4. Conclusions and discussions

Using a stochastic soil moisture model, this study investigates the impact of interannual variability of precipitation and potential evaporation on the long-term mean annual evapotranspiration as well as the interannual variability of evapotranspiration within the Budyko framework. The interannual variability of precipitation is further separated into the interannual variability of daily rainfall depth and the interannual variability of the frequency of daily rainfall events. The results indicate that the interannual variability of precipitation and potential evaporation reduces the long-term mean annual evapotranspiration given the same dryness index. This reduction effect is mostly prominent when the dryness index is within the range from 0.5 to 2. The maximum reductions in the evaporation ratio (i.e., the ratio of evapotranspiration to precipitation) can reach 8–10% for a range of coefficient of variation (CV) values for precipitation and potential evaporation. Our analysis reveals that the relations between the maximum reductions and the interannual variability of daily rainfall depth and the interannual variability of the frequency of daily rainfall events both follow power laws. But the sensitivity of maximum reductions to the interannual variability of daily rainfall depth ( $\alpha$ ) is different from that to the interannual variability of the frequency of daily rainfall events ( $\lambda$ ), which is due to their different roles in affecting the *pdf* of soil moisture. The relation between the maximum reductions and the interannual variability of potential evaporation also follows a power law. Hence, the larger the interannual variability of precipitation and potential evaporation becomes, the larger the reductions in the long-term mean annual evapotranspiration will be. As the interannual variability of precipitation and/or potential evaporation increases, the interannual variability of evapotranspiration also increases. It is shown that the interannual variability of daily rainfall depth and the frequency of daily rainfall events have quantitatively different impacts on the interannual variability of evapotranspiration when using the empirical curve proposed by Koster and Suarez [30] as a reference. They also interact differently with the interannual variability of potential evaporation.

The Budyko curve and the equations derived by Koster and Suarez [30] (which are also based on the Budyko curve) are frequently used in the literature to examine the long-term mean annual evapotranspiration and the interannual variability of evapotranspiration, respectively. In this study, the two are used as a reference to compare with our simulations. The Budyko curve, which was first proposed by Budyko as an empirical fit to observational data [18,19], is a simple representation of the land surface system to climate and has been verified over many places (e.g., see Li et al. [54] for applications of the Budyko curve over major global river basins). The reduction in the long-term mean annual

evapotranspiration induced by the interannual variability of precipitation and potential evaporation is linked to the concave nature of the Budyko curve. That is, the evaporation ratio inferred from the Budyko curve using the averaged dryness index  $(E/P)_a'$  is larger than the averaged evaporation ratio  $(E/P)_a$ . The concave nature of the Budyko curve is well captured by the stochastic soil moisture model (see Fig. 1). Note that altering values that are specified in Table 1 does not alter the concave nature of the resulting Budyko curve from the stochastic soil moisture model. Following Koster and Suarez [30], here we assume that the annual precipitation, potential evaporation and evapotranspiration also satisfy a Budyko-like curve. To simplify our illustration, only case 4 to case 1 are discussed. As shown in Fig. 9, a pair of constant  $\alpha$  and  $\lambda$  results in constant annual precipitation and thus the annual dryness index is always identical to  $(E_p/P)_a$ , which is the long-term mean dryness index. As such, the long-term mean annual evaporation ratio is  $(E/P)_a'$  in case 1 (see Fig. 9). For case 4 with variable  $\alpha$  and  $\lambda$ , the annual dryness index changes (e.g.,  $(E_p/P)_1$  and  $(E_p/P)_2$  for two different years on Fig. 9). The long-term mean dryness index remains  $(E_p/P)_a$  since the mean  $\alpha$  and  $\lambda$  are identical to those in case 1. Nevertheless, the long-term mean annual evaporation ratio is  $(E/P)_a = \frac{(E/P)_1 + (E/P)_2}{2}$  instead of  $(E/P)_a'$ . It is clear that  $(E/P)_a$  is lower than  $(E/P)_a'$  due to the concave nature of the Budyko-like curve, which is consistent with the reductions observed in Fig. 2. Hence as the interannual variability of precipitation and/or potential evaporation increases, the spread of  $E_p/P$  increases, leading to increases in the spread of  $E/P$  (i.e., increases in the interannual variability of evapotranspiration) while reductions in the average  $E/P$ . In addition, the concavity associated with the Budyko-like curve is mostly apparent when the dryness index is within the range of [0.5, 2], which explains the maximum reductions observed in this range in Fig. 2. A direct outcome of this analysis is that the Budyko curve at long-term scales should not be used at annual scales, since if the data follow a Budyko-like curve at annual scales, the long-term mean of these data will be below this Budyko-like curve.

The results presented in this study have some significant implications. For example, there has been growing evidence showing that the variability of precipitation is to increase under a changing climate [59–62] and extreme rainfall events and extreme droughts become more and more frequent in some areas [9,10,12]. One might then expect that the long-term mean annual evapotranspiration would be reduced and hence ecosystem productions such as the net primary production would be also reduced. Admittedly, there is still debate about the impact of climate change on precipitation [63]; nevertheless, this study certainly illustrates the potential impacts of increasing interannual variability of precipitation as well as potential evaporation on evapotranspiration as a result of climate change. The study also has some limitations that are

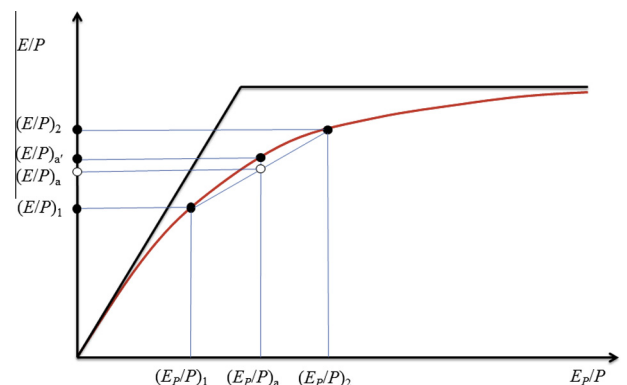


Fig. 9. A schematic figure illustrates the concave nature of the Budyko curve.

important to appreciate. First, the soil moisture model used in this study, despite its inclusion of many hydrological processes, remains a simplified model. Some processes such as infiltration-excess runoff are not considered and might play a non-negligible role [43]. Second, the vegetation response to changes in the inter-annual variability of precipitation is not considered. The dryness index under which the maximum reductions in  $E/P$  occur is not necessarily the conditions under which ecosystems are mostly sensitive to changes in  $E/P$ . The sensitivity of ecosystems to reductions in  $E/P$  also depends on the vegetation characteristics. Third, the simulations also do not account for interannual water storage changes and hence the conclusions might not be applicable for basins with significant human activities such as irrigation and groundwater extraction. Observational datasets or analyses based on more complicated numerical models are needed to further evaluate these effects.

## Acknowledgments

Support from the NOAA (U.S. Department of Commerce) grant NA08OAR4320752 and the Carbon Mitigation Initiative at Princeton University, sponsored by BP is acknowledged. The statements, findings, and conclusions are those of the author and do not necessarily reflect the views of the NOAA, the U.S. Department of Commerce or BP. I would like to thank Professor Ignacio Rodriguez-Iturbe from Princeton University for constructive suggestions. I also want to thank Maofeng Liu, Bo Guo and Ming Pan from Princeton University, Ruijie Zeng from University of Illinois at Urbana-Champaign, Xue Feng from Duke University, and Zhentao Cong from Tsinghua University for valuable discussions. The three reviewers whose comments have led to significant improvements of the manuscript are greatly acknowledged.

## References

- [1] Rodríguez-Iturbe I, Porporato A. *Ecohydrology of water-controlled ecosystems: soil moisture and plant dynamics*. Cambridge, UK; New York, NY, USA: Cambridge University Press; 2004.
- [2] Brutsaert W. *Hydrology: an introduction*. New York: Cambridge University Press; 2005.
- [3] Eagleson PS. *Ecohydrology: Darwinian expression of vegetation form and function*. Cambridge, UK; New York: Cambridge University Press; 2002.
- [4] Walther GR, Post E, Convey P, Menzel A, Parmesan C, Beebee TJC, et al. Ecological responses to recent climate change. *Nature* 2002;416:389–95. <http://dx.doi.org/10.1038/416389a>.
- [5] Holmgren M, Hirota M, van Nes EH, Scheffer M. Effects of interannual climate variability on tropical tree cover. *Nat Clim Change* 2013;3:755–8. <http://dx.doi.org/10.1038/Nclimate1906>.
- [6] Malhi Y, Wright J. Spatial patterns and recent trends in the climate of tropical rainforest regions. *Philos Trans R Soc Lond Ser B-Biol Sci* 2004;359:311–29. <http://dx.doi.org/10.1098/Rstb.2003.1433>.
- [7] Holmgren M, Stapp P, Dickman CR, Gracia C, Graham S, Gutierrez JR, et al. Extreme climatic events shape arid and semiarid ecosystems. *Front Ecol Environ* 2006;4:87–95. [http://dx.doi.org/10.1890/1540-9295\(2006\)004\[0087:Ecesaa\]2.0.Co;2](http://dx.doi.org/10.1890/1540-9295(2006)004[0087:Ecesaa]2.0.Co;2).
- [8] Huxman T, Snyder K, Tissue D, Leffler AJ, Ogle K, Pockman W, et al. Precipitation pulses and carbon fluxes in semiarid and arid ecosystems. *Oecologia* 2004;141:254–68. <http://dx.doi.org/10.1007/s00442-004-1682-4>.
- [9] O'gorman PA, Schneider T. The physical basis for increases in precipitation extremes in simulations of 21st-century climate change. *Proceedings of the national academy of sciences of the United States of America* 2009;106:14773–7. <http://dx.doi.org/10.1073/Pnas.0907610106>.
- [10] Easterling DR, Meehl GA, Parmesan C, Changnon SA, Karl TR, Mearns LO. Climate extremes: observations, modeling, and impacts. *Science* 2000;289:2068–74. <http://dx.doi.org/10.1126/Science.289.5487.2068>.
- [11] Feng X, Porporato A, Rodríguez-Iturbe I. Changes in rainfall seasonality in the tropics. *Nat Clim Change* 2013;3:811–5. <http://dx.doi.org/10.1038/Nclimate1907>.
- [12] Solomon S, Qin D, Manning M, Chen Z, Marquis M, Averyt KB, et al. *Climate change 2007: the physical science basis: contribution of working group I to the fourth assessment report of the intergovernmental panel on climate change*. Cambridge, New York: Cambridge University Press; 2007.
- [13] Brutsaert W. *Evaporation into the atmosphere: theory, history, and applications*. Dordrecht, Holland: Reidel; 1982.
- [14] Katul GG, Oren R, Manzoni S, Higgins C, Parlange MB. Evapotranspiration: a process driving mass transport and energy exchange in the soil–plant–atmosphere–climate system. *Rev Geophys* 2012;50. <http://dx.doi.org/10.1029/2011rg000366>.
- [15] Wang KC, Dickinson RE. A review of global terrestrial evapotranspiration: observation, modeling, climatology, and climatic variability. *Rev Geophys* 2012;50. <http://dx.doi.org/10.1029/2011rg000373>.
- [16] Yuan WP, Liu SG, Yu GR, Bonnefond JM, Chen JQ, Davis K, et al. Global estimates of evapotranspiration and gross primary production based on MODIS and global meteorology data. *Remote Sens Environ* 2010;114(2010):1416–31. <http://dx.doi.org/10.1016/j.rse.01.022>.
- [17] Tian HQ, Chen GS, Liu ML, Zhang C, Sun G, Lu CQ, et al. Model estimates of net primary productivity, evapotranspiration, and water use efficiency in the terrestrial ecosystems of the southern United States during 1895–2007. *Forest Ecol Manage* 2010;259:1311–27. <http://dx.doi.org/10.1016/j.foreco.2009.10.009>.
- [18] Budyko MI. *Evaporation under natural conditions*. Israel Program for Scientific Translations; [available from the Office of Technical Services, U.S. Dept. of Commerce, Jerusalem; 1963].
- [19] Budyko MI. *Climate and life*. New York: Academic Press; 1974.
- [20] Fu BP. On the calculation of the evaporation from land surface. *Sci Atmos Sin* 1981;5:23–31 (in Chinese).
- [21] Zhang L, Dawes WR, Walker GR. Response of mean annual evapotranspiration to vegetation changes at catchment scale. *Water Resour Res* 2001;37:701–8.
- [22] Zhang L, Hickel K, Dawes WR, Chiew FHS, Western AW, Briggs PR. A rational function approach for estimating mean annual evapotranspiration. *Water Resour Res* 2004;40. <http://dx.doi.org/10.1029/2003wr002710>.
- [23] Renner M, Bernhofer C. Applying simple water-energy balance frameworks to predict the climate sensitivity of streamflow over the continental United States. *Hydrol Earth Syst Sci* 2012;16:2531–46. <http://dx.doi.org/10.5194/Hess-16-2531-2012>.
- [24] Renner M, Seppelt R, Bernhofer C. Evaluation of water-energy balance frameworks to predict the sensitivity of streamflow to climate change. *Hydrol Earth Syst Sci* 2012;16:1419–33. <http://dx.doi.org/10.5194/Hess-16-1419-2012>.
- [25] Roderick ML, Farquhar GD. A simple framework for relating variations in runoff to variations in climatic conditions and catchment properties. *Water Resour Res* 2011;47. <http://dx.doi.org/10.1029/2010wr009826>.
- [26] van der Velde Y, Vercauteren N, Jaramillo F, Dekker SC, Destouni G, Lyon SW. Exploring hydroclimatic change disparity via the Budyko framework. *Hydrol Process* 2013;3. <http://dx.doi.org/10.1002/hyp.9949>. n/a–n/a.
- [27] Wang DB, Alimohammadi N. Responses of annual runoff, evaporation, and storage change to climate variability at the watershed scale. *Water Resour Res* 2012;48. <http://dx.doi.org/10.1029/2011wr011444>.
- [28] Wang DB, Hejazi M. Quantifying the relative contribution of the climate and direct human impacts on mean annual streamflow in the contiguous United States. *Water Resour Res* 2011;47. <http://dx.doi.org/10.1029/2010wr010283>.
- [29] Yang HB, Yang DW. Derivation of climate elasticity of runoff to assess the effects of climate change on annual runoff. *Water Resour Res* 2011;47. <http://dx.doi.org/10.1029/2010wr009287>.
- [30] Koster RD, Suarez MJ. A simple framework for examining the interannual variability of land surface moisture fluxes. *J Clim* 1999;12:1911–7. [http://dx.doi.org/10.1175/1520-0442\(1999\)012<1911:Asfiet>2.0.Co;2](http://dx.doi.org/10.1175/1520-0442(1999)012<1911:Asfiet>2.0.Co;2).
- [31] Milly PCD, Dunne KA. Macroscale water fluxes – 2. Water and energy supply control of their interannual variability. *Water Resour Res* 2002;38. <http://dx.doi.org/10.1029/2001wr000760>.
- [32] Potter NJ, Zhang L. Interannual variability of catchment water balance in Australia. *J Hydrol* 2009;369:120–9. <http://dx.doi.org/10.1016/j.jhydrol.2009.02.005>.
- [33] Donohue RJ, Roderick ML, McVicar TR. On the importance of including vegetation dynamics in Budyko's hydrological model. *Hydrol Earth Syst Sci* 2007;11:983–95.
- [34] Yang DW, Shao WW, Yeh PJF, Yang HB, Kanae S, Oki T. Impact of vegetation coverage on regional water balance in the nonhumid regions of China. *Water Resour Res* 2009;45. <http://dx.doi.org/10.1029/2008wr006948>.
- [35] Williams CA, Reichstein M, Buchmann N, Baldocchi D, Beer C, Schwalm C, et al. Climate and vegetation controls on the surface water balance: synthesis of evapotranspiration measured across a global network of flux towers. *Water Resour Res* 2012;48. <http://dx.doi.org/10.1029/2011wr011586>.
- [36] Shao QX, Traylen A, Zhang L. Nonparametric method for estimating the effects of climatic and catchment characteristics on mean annual evapotranspiration. *Water Resour Res* 2012;48. <http://dx.doi.org/10.1029/2010wr009610>.
- [37] Yang DW, Sun FB, Liu ZY, Cong ZT, Ni GH, Lei ZD. Analyzing spatial and temporal variability of annual water-energy balance in nonhumid regions of China using the Budyko hypothesis. *Water Resour Res* 2007;43. <http://dx.doi.org/10.1029/2006wr005224>.
- [38] Yokoo Y, Sivapalan M, Oki T. Investigating the roles of climate seasonality and landscape characteristics on mean annual and monthly water balances. *J Hydrol* 2008;357:255–69. <http://dx.doi.org/10.1016/j.jhydrol.2008.05.010>.
- [39] Ma ZM, Kang SZ, Zhang L, Tong L, Su XL. Analysis of impacts of climate variability and human activity on streamflow for a river basin in arid region of northwest China. *J Hydrol* 2008;352:239–49. <http://dx.doi.org/10.1016/j.jhydrol.2007.12.022>.
- [40] Budyko MI, Zubenok LI. Determination of evaporation from the land surface. *Izv Akad Nauk SSSR Ser Geogr* 1961;6:3–17 (in Russian).

- [41] Milly PCD. Climate, soil–water storage, and the average annual water-balance. *Water Resour Res* 1994;30:2143–56.
- [42] Feng X, Vico G, Porporato A. On the effects of seasonality on soil water balance and plant growth. *Water Resour Res* 2012;48. <http://dx.doi.org/10.1029/2011wr011263>.
- [43] Potter NJ, Zhang L, Milly PCD, McMahon TA, Jakeman AJ. Effects of rainfall seasonality and soil moisture capacity on mean annual water balance for Australian catchments. *Water Resour Res* 2005;41. <http://dx.doi.org/10.1029/2004wr003697>.
- [44] Huntington TG. Evidence for intensification of the global water cycle: review and synthesis. *J Hydrol* 2006;319:83–95. <http://dx.doi.org/10.1016/j.jhydrol.2005.07.003>.
- [45] Balan Sarojini B, Stott PA, Black E, Polson D. Fingerprints of changes in annual and seasonal precipitation from CMIP5 models over land and ocean. *Geophys Res Lett* 2012;39:21706. <http://dx.doi.org/10.1029/2012gl053373>.
- [46] Laio F, Porporato A, Ridolfi L, Rodriguez-Iturbe I. Plants in water-controlled ecosystems: active role in hydrologic processes and response to water stress – II. Probabilistic soil moisture dynamics. *Adv Water Resour* 2001;24:707–23. [http://dx.doi.org/10.1016/S0309-1708\(01\)00005-7](http://dx.doi.org/10.1016/S0309-1708(01)00005-7).
- [47] Salvucci GD. Estimating the moisture dependence of root zone water loss using conditionally averaged precipitation. *Water Resour Res* 2001;37:1357–65. <http://dx.doi.org/10.1029/2000WR900336>.
- [48] D'Odorico P, Ridolfi L, Porporato A, Rodriguez-Iturbe I. Preferential states of seasonal soil moisture: the impact of climate fluctuations. *Water Resour Res* 2000;36:2209–19. <http://dx.doi.org/10.1029/2000wr900103>.
- [49] Daly E, Porporato A. Impact of hydroclimatic fluctuations on the soil water balance. *Water Resour Res* 2006;42. <http://dx.doi.org/10.1029/2005wr004606>.
- [50] Porporato A, Laio F, Ridolfi L, Caylor KK, Rodriguez-Iturbe I. Soil moisture and plant stress dynamics along the Kalahari precipitation gradient. *J Geophys Res Atmos* 2003;108. <http://dx.doi.org/10.1029/2002jd002448>.
- [51] Ridolfi L, D'Odorico P, Porporato A, Rodriguez-Iturbe I. Impact of climate variability on the vegetation water stress. *J Geophys Res Atmos* 2000;105:18013–25. <http://dx.doi.org/10.1029/2000jd900206>.
- [52] Arora VK. The use of the aridity index to assess climate change effect on annual runoff. *J Hydrol* 2002;265:164–77. [http://dx.doi.org/10.1016/S0022-1694\(02\)00101-4](http://dx.doi.org/10.1016/S0022-1694(02)00101-4).
- [53] Donohue RJ, Roderick ML, McVicar TR. Assessing the differences in sensitivities of runoff to changes in climatic conditions across a large basin. *J Hydrol* 2011;406:234–44. <http://dx.doi.org/10.1016/j.jhydrol.2011.07.003>.
- [54] Li D, Pan M, Cong ZT, Zhang L, Wood E. Vegetation control on water and energy balance within the Budyko framework. *Water Resour Res* 2013;49:969–76. <http://dx.doi.org/10.1002/Wrcr.20107>.
- [55] Yang DW, Sun FB, Liu ZT, Cong ZT, Lei ZD. Interpreting the complementary relationship in non-humid environments based on the Budyko and Penman hypotheses. *Geophys Res Lett* 2006;33:L18402. <http://dx.doi.org/10.1029/2006gl027657>.
- [56] Porporato A, Daly E, Rodriguez-Iturbe I. Soil water balance and ecosystem response to climate change. *Am Nat* 2004;164:625–32.
- [57] Cong ZT, Zhang XY, Li D, Yang HB, Yang DW. Understanding hydrological trends by combining the Budyko hypothesis and a stochastic soil moisture model. *Hydrol Sci J*, in press.
- [58] Yang HB, Yang DW, Lei ZD, Sun FB. New analytical derivation of the mean annual water-energy balance equation. *Water Resour Res* 2008;44. <http://dx.doi.org/10.1029/2007wr006135>.
- [59] Chou C, Neelin JD, Chen CA, Tu JY. Evaluating the "rich-get-richer" mechanism in tropical precipitation change under global warming. *J Clim* 2009;22:1982–2005. <http://dx.doi.org/10.1175/2008jcli2471.1>.
- [60] Held IM, Soden BJ. Robust responses of the hydrological cycle to global warming. *J Clim* 2006;19:5686–99. <http://dx.doi.org/10.1175/Jcli3990.1>.
- [61] Seager R, Naik N, Vecchi GA. Thermodynamic and dynamic mechanisms for large-scale changes in the hydrological cycle in response to global warming. *J Clim* 2010;23:4651–68. <http://dx.doi.org/10.1175/2010jcli3655.1>.
- [62] Seager R, Naik N, Vogel L. Does global warming cause intensified interannual hydroclimate variability? *J Clim* 2012;25:3355–72. <http://dx.doi.org/10.1175/Jcli-D-11-00363.1>.
- [63] Wu PL, Christidis N, Stott P. Anthropogenic impact on Earth's hydrological cycle. *Nat Clim Change* 2013;3:807–10. <http://dx.doi.org/10.1038/Nclimate1932>.